Acta Tropica 185 (2018) 77–85

Contents lists available at ScienceDirect

Acta Tropica

journal homepage: www.elsevier.com/locate/actatropica

Space-time clusters and co-occurrence of chikungunya and dengue fever in Colombia from 2015 to 2016

M.R. Desjardins[a], A. Whiteman[a], I. Casas[b], E. Delmelle[a,*]

[a] Department of Geography and Earth Sciences and Center for Applied Geographic Information Science, University of North Carolina at Charlotte, 2901 University City Blvd, Charlotte, NC, 28223, United States

[b] School of History and Social Sciences, Louisiana Tech University, 305 Wisteria St, Ruston, LA, 71272, United States

ARTICLE INFO

Keywords:
Space-time statistics
Vector-borne diseases
Clusters
GIS
Colombia

ABSTRACT

Vector-borne diseases (VBDs) infect over one billion people and are responsible for over one million deaths each year, globally. Chikungunya (CHIK) and Dengue Fever (DENF) are emerging VBDs due to overpopulation, increases in urbanization, climate change, and other factors. Colombia has recently experienced severe outbreaks of CHIK AND DENF. Both viruses are transmitted by the *Aedes* mosquitoes and are preventable with a variety of surveillance and vector control measures (e.g. insecticides, reduction of open containers, etc.). Spatiotemporal statistics can facilitate the surveillance of VBD outbreaks by informing public health officials where to allocate resources to mitigate future outbreaks. We utilize the univariate Kulldorff space-time scan statistic (STSS) to identify and compare statistically significant space-time clusters of CHIK and DENF in Colombia during the outbreaks of 2015 and 2016. We also utilize the multivariate STSS to examine co-occurrences (simultaneous excess incidences) of DENF and CHIK, which is critical to identify regions that may have experienced the greatest burden of VBDs. The relative risk of CHIK and DENF for each Colombian municipality belonging to a univariate and multivariate cluster is reported to facilitate targeted interventions. Finally, we visualize the results in a three-dimensional environment to examine the size and duration of the clusters. Our approach is the first of its kind to examine multiple VBDs in Colombia simultaneously, while the 3D visualizations are a novel way of illustrating the dynamics of space-time clusters of disease.

1. Introduction

Vector-borne diseases (e.g. malaria, dengue fever, Zika, chikungunya, etc.) affect more than 1 billion people a year worldwide, cause over 1 million deaths, and cost hundreds of billions of dollars in societal costs (World Health Organization, 2014b). Mosquitoes are the most common vectors, responsible for transmitting a variety of arboviruses. The diversity of mosquito-borne pathogens (Beckham and Tyler 2015), a growing geographical vector range (Benedict et al., 2007; Rochlin et al., 2013), and a mid-century decline in vector control efforts (Floore 2006), have led to global increases in arbovirus disease transmission in recent decades (World Health Organization, 2014a). In regions where multiple pathogens are widespread, comprehensive efforts to understand the interaction of multiple disease outbreaks across a heterogeneous landscape can aid in outbreak prevention and response (Ochieng et al., 2013).

Recently, several particular pathogens, most notably Dengue Fever (DENF) and Chikungunya Virus (CHIK), have been responsible for the majority of the burden caused by mosquito-borne diseases (Wang et al., 2016). Both diseases are caused by viruses that are primarily transmitted by the *Aedes aegypti* mosquito (Harrington et al., 2001), with *A. albopictus* acting as a secondary vector (Gratz 2004; Tsetsarkin et al., 2007; Paupy et al., 2010; Chouin-Carneiro et al., 2016). These two species are peridomestic container-breeding mosquitoes that have become prolific in urban areas due to the widespread availability of breeding habitats (Tauil 2001; Powell and Tabachnick 2013). A combination of climate change (Liu-Helmersson et al., 2014), rapid urbanization (Tauil 2001), and globalization (Charrel et al., 2007) have expanded the vector's range and caused the two infectious diseases to emerge in novel regions.

DENF, which can be caused by any of the five known viral serotypes (DEN 1–5), is the most rapidly spreading arbovirus on Earth (Wilder-Smith et al., 2017). Over 40% of humans are at risk of transmission, with incidence rising 30-fold in the last 50 years; while it is estimated that there are approximately 390 million DENF infections annually (Bhatt et al., 2013). Additionally, the viruses have recently spread geographically to include novel outbreaks in Europe in 2010 and the United States in 2013 (Bhatt et al., 2013). CHIK had been restricted to

* Corresponding author.
E-mail address: eric.delmelle@uncc.edu (E. Delmelle).

https://doi.org/10.1016/j.actatropica.2018.04.023
Received 29 December 2017; Received in revised form 19 April 2018; Accepted 22 April 2018
Available online 27 April 2018
0001-706X/ © 2018 Elsevier B.V. All rights reserved.

Africa, Southeast Asia, and India prior to 2013 when it was first detected in the Americas and Caribbean. In the subsequent 2013–2015 CHIK epidemic in the Americas, an estimated 39.5 million people were infected and an estimated societal cost of US$185 billion was incurred (Bloch 2016; Shepard 2010). Worries remain about potential novel regions becoming infected as well as the risk of antibody-dependent enhancements among populations with a history of hosting other arboviruses (Dejnirattisai et al., 2016; Kawiecki and Christofferson, 2016; Durbin 2016).

While the viruses that cause the abovementioned diseases are all closely related and share many epidemiological and clinical characteristics (Hanley and Weaver, 2008; Beckham and Tyler 2015), it is important to understand how different VBD outbreaks relate to each other in space and time, and where space-time clusters of different VBDs co-occur, especially since co-infection is possible (Rodriguez-Morales et al., 2016). Identifying and visualizing the space-time co-occurrence of multiple VBD clusters can shed light on which regions suffer the greatest burden of disease, helping decision-makers prioritize where to allocate resources.

Identifying and mapping disease outbreaks in space and time can provide information that can be useful in planning public health interventions (Peterson 2014; Pigott et al., 2015; Hay et al., 2013). Monitoring and analyzing outbreaks under critical space-time conditions can increase the efficiency of public health responses (Kitron 1998; Kitron 2000; Eisen and Eisen, 2011; Jacquez et al., 2005; Rogerson and Yamada 2008). Space-time analytics are particularly salient to estimate the dynamics of vector-borne diseases (Eisen and Lozano-Fuentes 2009), such as the rate of disease spread, cyclic pattern, direction, intensity, and risk of diffusion to new regions.

There are a number of different methods available that can quantify the spatiotemporal clustering of diseases cases. The space-time Ripley's *K* function evaluates the distribution of events to determine the magnitude of clustering at different spatial and temporal distances (Bailey and Gatrell 1995). The space-time Knox test identifies statistically significant case clusters at defined spatial and temporal distances (Kulldorff and Hjalmars 1999). The Mantel Index (Mantel 1967) addresses the limitations of the Knox test by assigning higher weight to nearby events both spatially and temporally. Using information from these previous tests, space-time patterns of diseases can then be visualized. For example, space-time kernel density estimation (STKDE), which is an extension of the traditional kernel density estimation (Silverman 1986), can help visualizing disease "hotspots" in both space and time, resulting in heat volume instead of heat maps (Brunsdon et al., 2007; Nakaya and Yano 2010). The space-time Knox test, Mantel Index, space-time Ripley's K function, and STKDE have all been used to map and monitor vector-borne disease outbreaks, including Dengue fever (Delmelle et al., 2013; Delmelle et al., 2014; Hohl et al., 2016), West Nile (Theophilides et al., 2003), Rift Valley Fever (Métras et al., 2012), and Chikungunya (Nsoesie et al., 2015).

One of the most common statistical methods used to identify the clusters of cases which define an outbreak are scan statistics. Scan statistics work by determining whether the number of cases found in a defined area exceeds what would be expected based on baseline conditions, such as host population size in the case of vector-borne disease. One can incorporate a temporal dimension by using space-time scan statistics. This allows for the identification of both the size and duration of statistically significant disease clusters across a given area. Here, we use Kulldorff's univariate and multivariate space-time scan statistics (STSS) (Kulldorff et al., 2005; Kulldorff et al., 2007), which employs moving cylinders across a plane to estimate the space-time clustering of aggregated data. The number of observed cases are then compared to the number of expected cases (e.g. disease rates per geographic unit).

Multivariate STSS can identify space-time clusters of multiple diseases that occur simultaneously (Jonsson et al., 2010; Perez et al., 2011; Greene et al., 2012; Amin et al., 2014). For example, Amin et al. (2014) used multivariate STSS to identify simultaneous clusters of three different pediatric cancers in Florida. While univariate STSS have been used to examine VBD outbreaks, such as West Nile (Lian et al., 2007; Mulatti et al., 2015), Malaria (Gaudart et al., 2006; Coleman et al., 2009), Lyme Disease (Li et al., 2014), Chikungunya (Nsoesie et al., 2015), and Dengue fever (Schmidt et al., 2011; de Melo et al., 2012; Li et al., 2012; Banu et al., 2014), the literature lacks a study that utilizes multivariate STSS to examine simultaneous outbreaks of mosquito-borne diseases.

Many studies that utilize STSS generally visualize the results in 2D using small multiples (Naish et al., 2011; Banu et al., 2012; Uittenbogaard and Ceccato, 2012; Wang et al., 2014; Mulatti et al., 2015), failing to visualize the true space-time patterns of the clusters. The literature is scarce regarding the 3D visualization of space-time clusters reported from space-time scan statistics. Nakaya and Yano (2010) and Cheng and Williams (2012) visualized the space-time clusters of crime in Kyoto, Japan and London within a 3D-environment; and Cheng and Wicks (2014) visualized space-time clusters of tweets related to multiple events in London in a space-time cube (3D). These papers demonstrated the effectiveness of integrating 3D visualization, showing the temporal variation of clusters that 2D techniques inhibit, for example. Conversely, visualizing space-time clusters of disease in a 3D environment can improve the understanding of the space-time dynamics of an epidemic, such as variations in duration and size, and how clusters move through time, the co-occurrence of multiple VBDs, and reoccurrence of significant clusters.

For this paper, both univariate and multivariate STSS are utilized to identify statistically significant space-time clusters of CHIK and DENF in Colombia during the outbreaks occurring in 2015 and 2016, including the co-occurrence between both VBDs. We report a variety of statistics, including the observed and expected cases, relative risk, and others. The results are visualized in both 2D and 3D to examine the size and duration of the reported space-time clusters. To our knowledge, this is the first study to apply space-time statistics to identify clusters of multiple VBDs in Colombia, while facilitating targeted interventions by comparing the relative risk of CHIK and DENF in municipalities that belong to significant space-time clusters. Notably, this is also the first study that applies a multivariate space-time scan approach to identify significant co-occurrence of multiple VBDs. Furthermore, the 3D visualizations illustrate the dynamics of the space-time clusters, which cannot be depicted by using solely 2D techniques. The findings in this exploratory analysis can help public health officials prioritize resource allocation to potentially mitigate future outbreaks of CHIK and DENF in Colombia.

The remainder of this paper is structured as follows: Section 2 describes the data for DENF and CHIK in Colombia, and the methods utilized to identify significant space-time clusters and visualize the subsequent results in both 2D and 3D. Section 3 compares the results, such as the size and duration of the space-time clusters for each VBD. Finally, Section 4 provides a discussion and concluding remarks, including limitations of this study and potential future avenues of research.

2. Data and methods

2.1. Data

Case data for DENF and CHIK were obtained from SIVIGILA (Sistema Nacional de Vigilancia en Salud Pública – National Public Health Surveillance System).[1] SIVIGILA is a system administered by the National Institute of Health of Colombia (Instituto Nacional de Salud – INS) which provides information regarding events that can affect the health of the Colombian population in a systematic and timely manner.

[1] http://www.ins.gov.co/lineas-de-accion/Subdireccion-Vigilancia/sivigila/Paginas/sivigila.aspx (last accessed: 30 Mar 2018).

Data is uploaded into the SIVIGILA system on a weekly basis by UPGDs (from their acronym in Spanish: Unidades Primarias Generadoras de Datos – Data Generating Primary Units). UPGDs are defined as any private or public entity that diagnoses the occurrence of a public health event of interest and is required to report the necessary information regarding the event, in order to meet the goals of SIVIGILA (INS, 2016a).

The data is used to generate alerts and responses to public health events. The INS reports are made available through Routine Surveillance webpages of all the diseases they record data for (yearly summaries; INS, 2016b). The summaries contain weekly disease cases for each municipality, where both suspicious, probable, and confirmed cases are included. For DENF, a probable case is identified as exhibiting fever with two or more of the following symptoms: headache, retroocular pain, myalgia, arthralgia, and rash (INS, 2017a). For CHIK, a suspicious case is identified as a patient residing or visiting 8–15 days prior to the onset of symptoms in a municipality where there have not been laboratory cases of CHIK confirmed, running a fever over 38 °C, arthralgia or arthritis, uniform erythema, or symptoms that cannot be explained by other medical conditions (INS, 2017b). The INS describe the data as dynamic, subject to analysis and adjustment. Population data was obtained from the Geographic Information System for Planning Land Use Ordering of Colombia (SIGOT: Sistema de Información Geográfica para la Planeación y Ordenamiento Territorial).[2] Data correspond to the total number of individuals in 2015 and 2016, for each municipality.

2.2. Methods

We use the Kulldorff univariate space-time scan statistic (Kulldorff et al., 2005) in SaTScan™ to identify statistically significant space-time clusters of DENF and CHIK for 2015 and 2016. The statistic employs moving cylinders that scan the study area for potential space-time clusters of cases, while the base of the cylinder is the spatial dimension and the height reflects the temporal dimension. The center of the cylinder is defined as the centroid of each Colombian municipality and each cylinder is expanded until a maximum spatial and temporal size is reached (each cylinder is a potential cluster).

Using the discrete Poisson probability model, VBD cases are assumed to be Poisson distributed according to the at-risk population in Colombia. Our null hypothesis stipulates that the model reflects an inhomogeneous Poisson process with an intensity μ, which is proportional to the at-risk population. The alternative hypothesis is that the number of VBD cases exceeds the number of expected cases derived from the null model. A maximum likelihood ratio test is utilized to evaluate the null and alternative hypotheses, which is defined in Eq. (1):

$$\frac{L(Z)}{L_0} = \frac{\left(\frac{n_Z}{\mu(Z)}\right)^{n_Z}\left(\frac{N-n_Z}{N-\mu_{(Z)}}\right)^{N-n_Z}}{\left(\frac{N}{\mu(A)}\right)^{N}} \quad (1)$$

Where $L(Z)$ is the likelihood function for cylinder Z, while L_0 is the likelihood function for the null hypotheses for cylinder Z. Essentially, the number of observed VBD cases in a cylinder n_Z is divided by the number of expected cases in a cylinder $\mu(Z)$ to the power of the observed n_Z, multiplied by the observed cases divided by the expected cases outside of the cylinder. The numerator is then divided by the quotient of dividing the total number of observed cases for the entire study area N across all time periods $\mu(A)$, to the power of the total number of observed cases. The cylinder will have an elevated risk if the likelihood ratio is greater than 1. Furthermore, the space-time scan statistic uses different cylinder sizes, and the cylinder with the highest likelihood ratio (maximum) is the most likely cluster.

To identify the co-occurrence (simultaneous excess incidence) of DENF and CHIK outbreaks during our study period, we utilize the multivariate space-time Poisson scan-statistic (Kulldorff et al., 2007). As with the univariate statistic, the log likelihood ratio (LLR) for each disease is computed within each cylinder. The multivariate statistic sums the LLRs for both DENF and CHIK in a particular cylinder, producing a new LLR for that cylinder. Finally, the maximum summed LLR is reported as the most likely cluster, which is defined in Eq. (2):

$$T = \max_z \sum_i LLR_i(Z) \quad (2)$$

Where T is the most likely cluster and i is the dataset for a particular disease within cylinder Z.

Each reported cluster has a minimum temporal length of two weeks. The maximum spatial and temporal size of the space-time cylinders was set at 25% of the population at-risk and 25% of the study period, respectively. Monte Carlo simulations (n = 999) were performed for each model run to assess the statistical significance of the observed clusters. Subsequently, we report clusters that have a p-value less than 0.05 with no geographical overlap (most likely and secondary clusters). Finally, we map the relative risk of CHIK and DENF for each municipality belonging to a univariate and multivariate cluster. Relative risk quantifies the risk of becoming infected with a disease in one location compared to all other locations, which is defined in Eq. (3):

$$RR = \frac{c/e}{(C-c)/(C-e)} \quad (3)$$

Where c is the total number of observed cases in a municipality, e is the total number of expected cases in a municipality (proportional to at-risk population), and C is the total number of observed cases in Colombia.

3. Results

3.1. Univariate: CHIK

During the CHIK outbreaks in Colombia between 2015 and 2016, a total of n = 2755 and n = 8417 cases were reported, respectively (n = 11,172 combined). The temporal distribution of CHIK cases is shown in Fig. 1. January 2015 recorded the highest number of cases (n = 556), while the first half of the year contained the majority of cases, with a sharp decline after April 2015. The CHIK epidemic saw an exponential increase of cases starting in January 2016, while that month also experienced the maximum for that year with n = 1362 cases. The number of cases remained elevated until June 2016 when it started to decline.

Seven clusters affecting 572 municipalities were reported for CHIK (Fig. 2A) and the results are summarized in Table 1. Three clusters were reported in 2015 with centers in (4) Valledupar: weeks 1–2, (5) Unguía: weeks 1–5, and (7) San Zenón: weeks 5–6. In 2016, four clusters were reported with centers in (1) Nátaga: weeks 53–78, (2) Santa Rosalía: weeks 56–79, (3) Uramita: weeks 61–81, and (6) Córdoba: weeks 53–55; and the municipality of Cali is located in cluster 1, which contained the most observed cases (n = 1614). Clusters 6 and 7 do not have a radius, meaning that the cluster was contained within the municipalities of Valledupar and Córdoba, respectively. Cluster 6 also had the highest relative risk due to the very low expected number of cases, while cluster 1 had the longest duration of twenty-five weeks, which is also the most likely cluster. Generally, clusters of CHIK containing municipalities with low population densities reported a higher relative risk. Notably, the CHIK clusters in 2016 had substantially longer durations than those reported in 2015.

Fig. 3A depicts the relative risk for each municipality belonging to a significant space-time cluster of CHIK. Out of the 572 municipalities assigned to a cluster, 283 reported a relative risk of 0 (no observed cases), and 107 contained a relative risk between 0 and 1 (lower

[2] http://sigotn.igac.gov.co/sigotn/frames_pagina.aspx (last accessed: 30 Mar 2018).

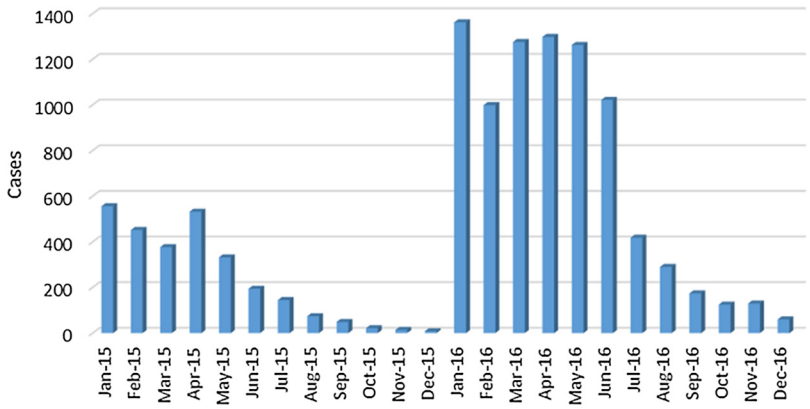

Fig. 1. Temporal distribution of CHIK in Colombia for 2015 and 2016.

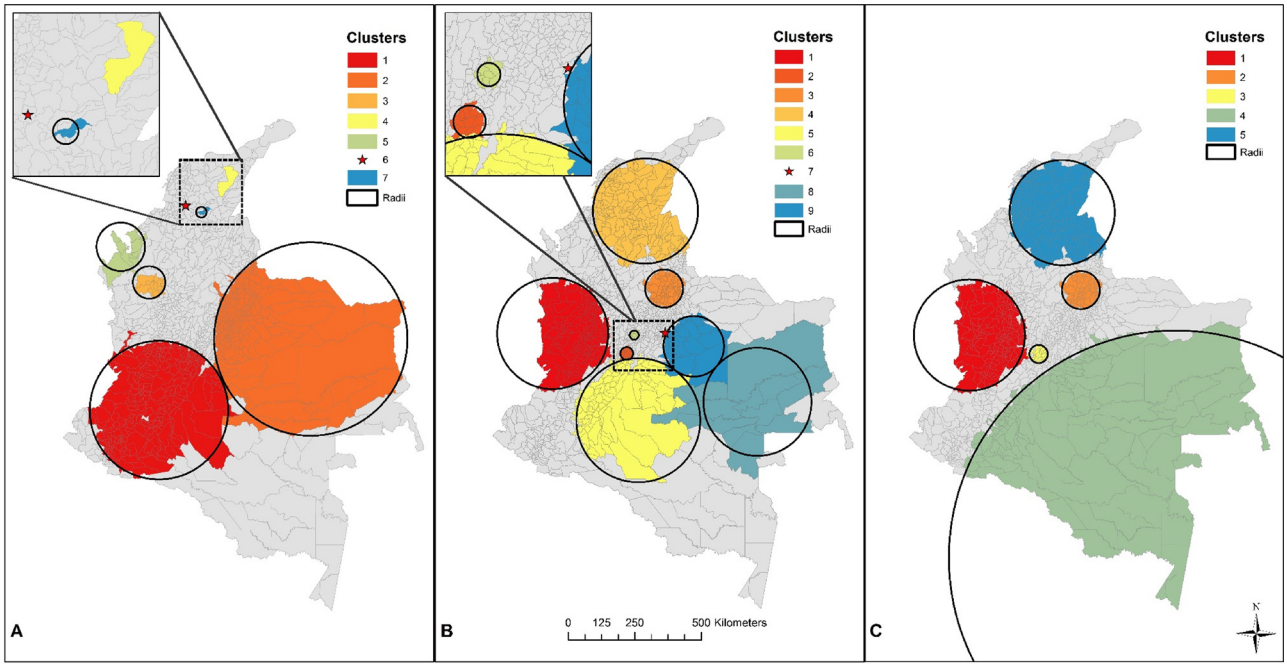

Fig. 2. Clusters of (A) CHIK, (B) DENF, and (C) multivariate.

Table 1
CHIK Clusters.

Cluster	Duration (weeks)	p-value	Observed	Expected	Relative Risk	Municipalities
1	53–78	$p < 0.01$	3818	694.5	7.8	271
2	56–79	$p < 0.01$	2145	250.9	10.3	269
3	61–81	$p < 0.01$	110	8.3	13.3	18
4	1–2	$p < 0.01$	30	2.0	14.9	1
5	1–5	$p < 0.01$	44	7.2	6.2	10
6	53–55	$p < 0.01$	10	0.08	122.15	1
7	5–6	$p < 0.01$	5	0.12	42.62	2

observed than expected cases). Conversely, 182 municipalities have a relative risk greater than 1 (higher observed than expected cases), while San Luis de Gaceno in cluster 2 reported the highest relative risk of 52.8. For cluster 1, San José del Fragua has the highest relative risk (RR = 37.9), 55 municipalities reported a relative risk greater than 3, and Cali contained a relative risk of 3.9.

Fig. 4 visualizes the 2015 and 2016 clusters of CHIK in a 3D environment. The two y-axes are necessary to interpret the temporal dimension, while labels were added to highlight the duration of each cluster. A series of black rings were added to each cluster to reinforce the visualization, while each ring represents a particular week during 2015 and 2016. Fig. 4 shows three clusters occurring in 2015, followed by cluster 6 lasting for three weeks in January 2016, and three large clusters that have the longest durations during the two-year study period. Fig. 4 also shows how CHIK was predominately in northern Colombia in 2015, and then appeared in the South in 2016.

3.2. Univariate: DENF

During the DENF outbreaks in Colombia between 2015 and 2016, a

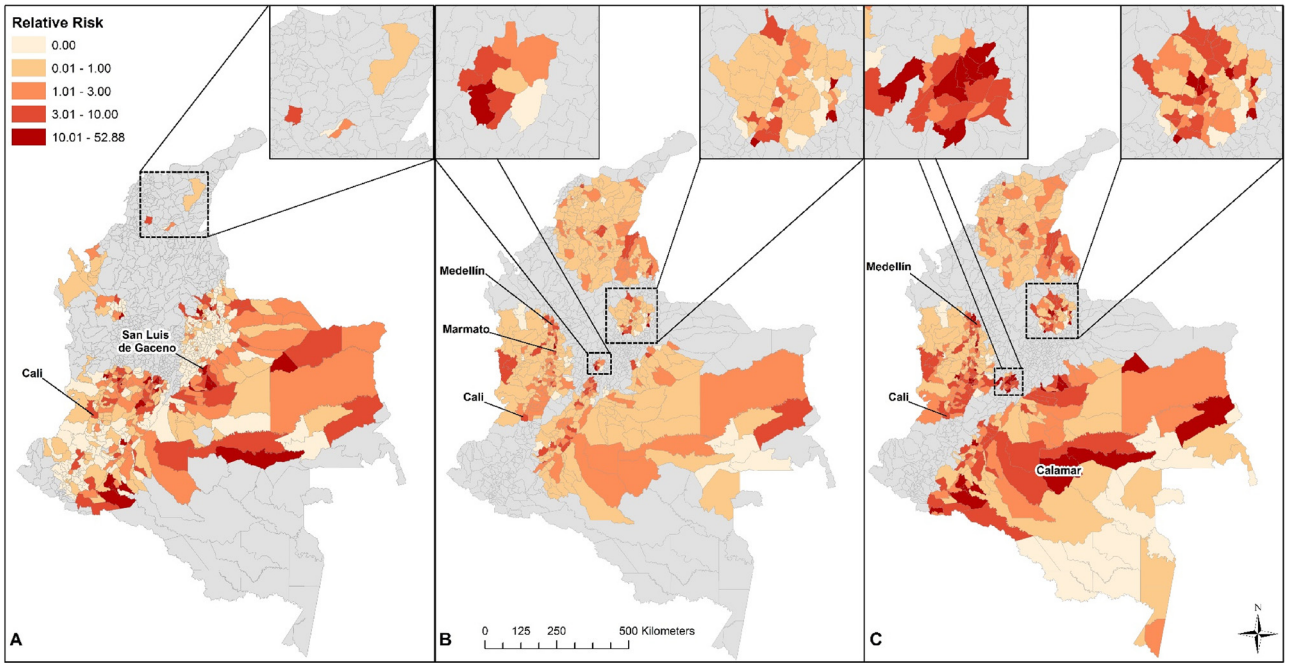

Fig. 3. Statistically significant relative risk per municipality for the (A) CHIK, (B) DENF, and (C) multivariate clusters.

total of n = 32,712 and n = 45,061 cases were reported, respectively (n = 77,773 combined). The temporal distribution of DENF cases is shown in Fig. 5. In 2015, January experienced the highest number of cases (n = 3900), while the remainder of the year saw over n = 2000 cases each month, followed by a slight decline in December. At the start of 2016, there was a rapid increase in DENF cases, with the peak of the epidemic occurring in March (n = 6668 cases). The number of cases remained high in the rainy season months, followed by a sharp decline starting in July 2016.

Nine clusters affecting 542 municipalities were reported for DENF (Fig. 2B), and the results are summarized in Table 2. Two clusters were reported in 2015 with centers in (4) Chimichagua: weeks 24–49, and (9) Maní: weeks 3–16. In 2016, seven clusters were reported with centers in (1) Medio Baudó: weeks 54–79, (2) Viotá: weeks 53–77, (3) Barichara: weeks 53–78, (5) La Macarena: weeks 53–62, (6) Supatá: weeks 53–73, (7) Miraflores (no radius): weeks 53–67, and (8)

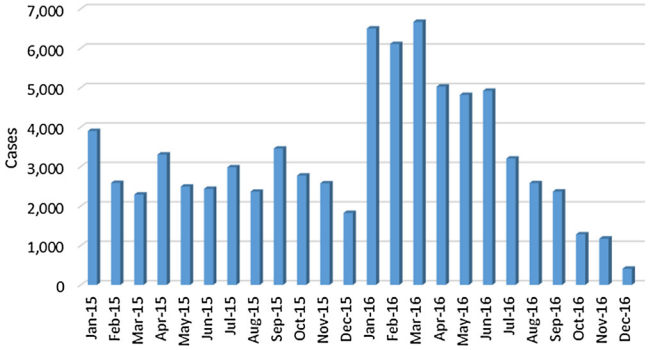

Fig. 5. Temporal distribution of DENF in Colombia for 2015 and 2016.

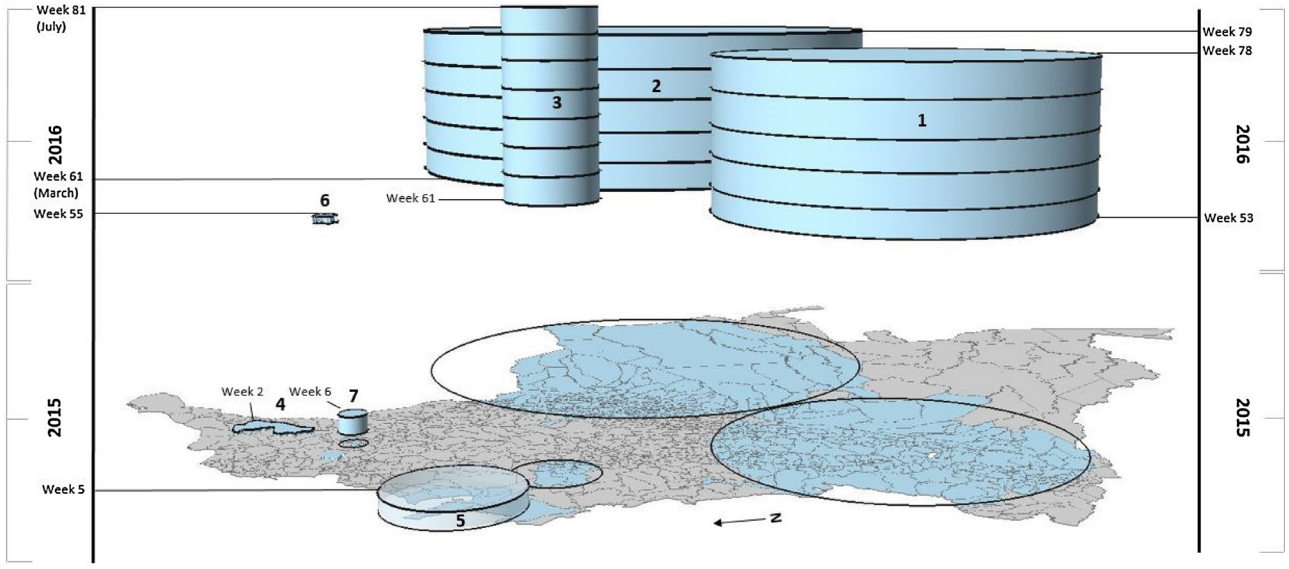

Fig. 4. 3D visualization of space-time CHIK clusters in Colombia from 2015 to 2016.

Table 2
DENF Clusters.

Cluster	Duration (weeks)	p-value	Observed	Expected	Relative Risk	Municipalities
1	54–79	$p < 0.01$	20,453	4,881.7	5.3	170
2	53–77	$p < 0.01$	1577	118.8	13.5	12
3	53–78	$p < 0.01$	2892	635.0	4.7	62
4	24–49	$p < 0.01$	4497	2,164.0	2.1	161
5	53–62	$p < 0.01$	1469	428.7	3.47	93
6	53–73	$p < 0.01$	243	28.57	8.5	7
7	53–67	$p < 0.01$	70	2.2	31.1	1
8	53–71	$p < 0.01$	61.0	3.5	3.5	11
9	3–16	$p < 0.01$	182	82.3	2.2	25

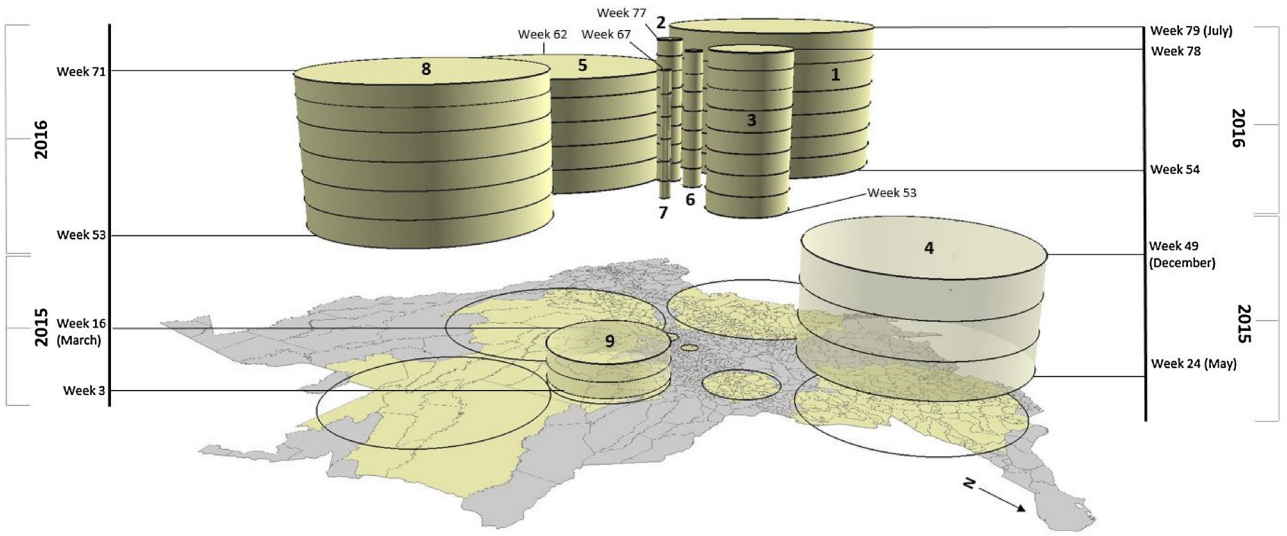

Fig. 6. 3D visualization of space-time DENF clusters in Colombia from 2015 to 2016.

Mapiripana: weeks 53–71; while the municipality Medellín in cluster 1 contained the most observed DENF cases (n = 11,582). Clusters 1, 3, and 4 had the longest duration (twenty-five weeks), while cluster 7 had the highest relative risk and lowest expected number of DENF cases. Fig. 6 visualizes the 2015 and 2016 clusters of DENF in a 3D environment. Similar to Fig. 4, the space-time dynamics of the DENF clusters are depicted; showing two clusters occurring during different weeks in 2015, followed by seven clusters in 2016 between weeks 53 and 79.

Fig. 3B depicts the relative risk for each municipality belonging to a significant space-time cluster of DENF. Out of the 544 municipalities assigned to a cluster, 39 reported a relative risk of 0, and 320 contained a relative risk between 0 and 1. Conversely, 185 municipalities have a relative risk greater than 1, while Soatá in cluster 3 reported the highest relative risk of 31.6. For cluster 1, Marmato has the highest relative risk (RR = 20.9), 20 municipalities reported a relative risk greater than 3, and Medellín contained a relative risk of 3.3.

3.3. Multivariate: co-occurrence of CHIK & DENF

Fig. 2C shows multivariate space-time clusters of CHIK and DENF in Colombia during the 2015 and 2016 epidemics. Five clusters affecting 539 municipalities were reported and Table 3 summarizes the results. One cluster was reported in 2015 with its center in (5) Chimichagua: weeks 24–49. In 2016, four clusters were reported with centers in (1) Medio Baudó: weeks 54–79, (2) Barichara: weeks 53–78, (3) Tocaima: weeks 53–76, and (4) Tarapacá: weeks 53–73; while the municipalities of Cali and Medellín are located in cluster 1. Fig. 7 provides a 3D visualization of the multivariate clusters. Cluster 5 in 2015 and clusters 1 and 2 in 2016 had the longest durations of twenty-five weeks each. Clusters 1–4 contained both CHIK and DENF, while cluster 5 only contained DENF. Although CHIK cases are found in cluster 5, there was not enough evidence to constitute a significant space-time cluster. In general, there are more observed DENF cases than CHIK in each cluster, however, a higher relative risk was reported for CHIK (exception of cluster 1) due to the lower amount expected cases. Furthermore, cluster 3 contained the highest combined relative risk (26.8).

Fig. 3C depicts the relative risk for each municipality belonging to a significant space-time multivariate clusters of CHIK and DENF. Out of the 541 municipalities assigned to a cluster, 40 reported a combined relative risk of 0, and 222 contained a combined relative risk between 0 and 1. Conversely, 279 municipalities have a relative risk greater than 1, while Calamar in cluster 4 reported the highest relative risk of 39.4. For cluster 1, Sopetrán has the highest relative risk (RR = 28.9), 58 municipalities reported a relative risk greater than 3, and Cali and Medellín have relative risks of 6.3 and 3.5, respectively.

In comparison with the univariate results, multivariate clusters 1 and 5 are in the same location and contain the same municipalities as DENF clusters 1 and 4. Multivariate cluster 1 also contains portions of CHIK cluster 3. Multivariate cluster 4 encompasses many of the municipalities belonging to CHIK clusters 1 and 2, and DENF clusters 5, 8, and 9. Furthermore, multivariate cluster 3 contains nine more municipalities than DENF cluster 2. Notably, CHIK cluster 5 and DENF cluster 6 were not found in a multivariate cluster; while CHIK clusters 4, 6, and 7 were not included in multivariate cluster 5. The differences in the spatial and temporal characteristics between the multivariate and univariate clusters can be attributed to the better statistical power and properties of the multivariate STSS (e.g. variance-covariance structure; Amin et al., 2014). Furthermore, the univariate results shed light on the spatial and temporal variations of CHIK and DENF. Examining the diseases independently can highlight regions where CHIK is more of a burden than DENF, and vice versa (e.g. CHIK cluster 5); while the multivariate results highlight regions significantly affected by both

Table 3
Multivariate Clusters.

Cluster	Duration (weeks)	Municipalities	p-value	VBD	Observed	Expected	Relative Risk
1	54–79	170	$p < 0.01$	CHIK	2515	698.2	4.3
				DENF	20,453	4,860.5	5.3
2	53–78	62	$p < 0.01$	CHIK	1366	90.9	16.9
				DENF	2892	633.2	4.7
3	53–76	21	$p < 0.01$	CHIK	439	26.6	17.1
				DENF	1763	185.4	9.7
4	53–73	125	$p < 0.01$	CHIK	1451	150.2	10.9
				DENF	2302	1,045.7	2.2
5	24–49	161	$p < 0.01$	CHIK	N/A	N/A	N/A
				DENF	4497	2,174.9	2.1

CHIK and DENF. Further analysis is needed to understand the complex local variations of humans, vectors, and viruses.

4. Discussion

The northern region of Colombia (including the Caribbean municipalities) was most affected by CHIK in 2015, while the southern region contained the largest clusters in 2016. Health officials dispatched to this region listed the possible causes as: (1) lack of education in avoiding mosquito breading sites, (2) poor neighborhoods lacking proper sewer systems, and (3) lack of laboratories to conduct the proper testing (Chachareros 2015), though broader scale assessments of vectorial capacity are needed to understand primary causes of cluster occurrence. In the case of DENF, for 2016 the Valle del Cauca department contributed more than 25% of the cases in Colombia (cluster 1). The city of Cali is the capital of this department and a known as an endemic region for the dengue virus (Noticiascaracol 2016). While both DENF and CHIK were generally widespread across Colombia in 2015–2016, there are unique spatial and temporal patterns evident between the two diseases. Temporally, the four multivariate clusters that contained co-occurrence of CHIK and DENF were found between January 2016 and July 2016. This coincides with the spikes in monthly totals of cases reported for each disease and indicates that seasonal factors may influence their co-occurrence.

There was no co-occurrence of DENF and CHIK in 2015, which also coincided with lower monthly totals of cases compared to 2016. Further studies will be needed to determine the reasons for the differences between years, although climatic shifts (Eastin et al., 2014; Hii et al., 2016), changes in vector control (Ooi et al., 2006), and changes in reporting (Shepard et al., 2014; Silva et al., 2016) have been known to cause fluctuations in year to year infection rates. It has also been noted that DENF follows a cyclical pattern manifesting as an epidemic every 2–3 years (Cali 2010). Clusters for both diseases coincided with regions of expected vector presence. The clusters are partially a consequence of the geography of Colombia. Of the 1123 municipalities, 829 have climatic conditions that are favorable for *Aedes* to reproduce (EPS C, 2015).

All clusters are centered on regions within the known precipitation, temperature, and elevation ranges of the vector. *Aedes* are rarely found above 1700m, and thus, municipalities within a cluster above the aforementioned elevation reflects a consequence of the Kulldorff method rather than the occurrence of local transmission. This results from cylinders being the base shape for the scanning operation, meaning that the reported clusters can sometimes include municipalities with low rates or where transmission did not actually occur. In general, it is unlikely that the municipalities above 1700 m hosted local transmission, yet they may host travel-related cases. Unfortunately, the dataset does not indicate whether cases were suspected of being transmitted elsewhere other than the reporting municipality. However, we circumvent the elevation issue by reporting relative risk for each

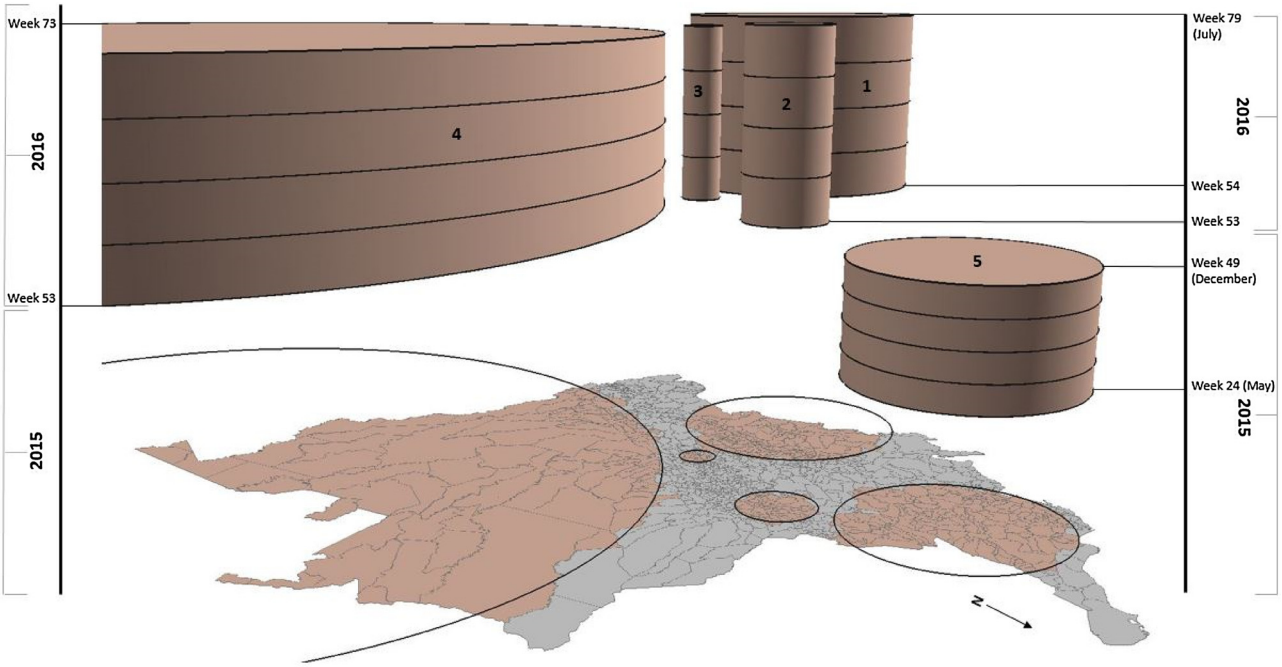

Fig. 7. 3D visualization of space-time multivariate clusters in Colombia from 2015 to 2016.

municipality, where every location above 1700 m has a relative risk of less than 1. Reporting relative risk for each municipality also reduces the uncertainty of solely reporting the locations belonging to a significant space-time cluster and facilities targeted interventions.

Coinfection of CHIK and DENF has been recognized across the global ranges of both diseases (Furuya-Kanamori et al., 2016). It is a common phenomenon in the multivariate clusters, and yet, no clinical significance of coinfection has been observed. However, there is concern that antibody-dependent enhancement may increase one's chance of contracting one disease after having previously been exposed to the other (Dejnirattisai et al., 2016). Both diseases are considered to be emerging VBDs. Thus, with low levels of immunity in newly exposed regions, the capacity for coinfection remains high (Furuya-Kanamori et al., 2016). DENF and CHIK represent a challenge to health authorities given that their clinical symptomatology presents very similarly and can be difficult to identify (Alvis-Guzmán et al., 2017). While DENF has been in the Americas for over 200 years, CHIK was first reported in the Americas in 2014 (Leparc-Goffart et al., 2014). By the end of that year, 82,588 cases were eventually recorded in Colombia. Our dataset represents the two years after that initial year, when immunity was first present in the population, and thus the rate of infection may be more representative of the long term. While the objective of our study was to identify the existence of case clusters in space and time, we invite consequent studies to investigate epidemiological conditions within each cluster to determine root causes for their occurrence. Efforts should include examinations of both vectorial capacity as well as host characteristics and variations in vector control.

5. Conclusion

Our paper successfully identified significant univariate and multivariate space-time clusters of DENF and CHIK in Colombia during the outbreaks in 2015 and 2016, while discussing some of the processes which were responsible for the epidemics. The reported clusters and the relative risk of each disease for each municipality were effectively visualized in both 2D and 3D, which complement each other and should be integrated in a space-time analysis of infectious diseases, improving the understanding of an epidemic. The 3D visualizations are especially effective at showing the space-time dynamics of the clusters, including the size, duration, and movement over time. Identifying the space-time co-occurrence of DENF and CHIK via multivariate STSS is another main contribution of this paper, which sheds light on the regions in Colombia that were hotspots for simultaneous VBD outbreaks. The approaches described in this paper can be utilized to identify high-risk areas, facilitating the implementation of targeted interventions to mitigate future outbreaks, such as reducing the number of potential breeding sites (e.g. open containers) for *Aedes*, and allocating improved public health resources. The areas of co-occurrence particularly require closer examination about why clusters of DENF and CHIK intersect in space and time. The approaches are also easily transferable to other study areas, acting as a universal toolset to study space-time clustering of infectious disease, and other phenomena such as crime.

Despite our study's strengths, there are a variety of limitations and avenues for future research. First, a cluster's relative risk reported by the scan statistic does not consider sociodemographic variations within the radius. For example, children and the elderly have the highest proportion of CHIK and DENF related deaths, while relative abundance may be related to socioeconomic variation. Therefore, the statistic could consider key sociodemographic factors (e.g. adjusted rates based on socioeconomic status), potentially generating more accurate relative risk estimates does not contain (the dataset used in this paper is aggregated and does not discriminate among gender or age groups). Second, the cylindrical shape of the clusters is likely not the true boundary of outbreaks (Kulldorff et al., 2005), while some of the reported clusters extended beyond the boundary of Colombia. We suggest that future investigations utilize other scanning methods (e.g. irregular shapes; Duczmal and Assuncao 2004; Tango and Takahashi, 2005; Ullah et al., 2017) to mitigate this concern. Finally, the data used is constantly revised by the National Institute of Health based on information reported by municipalities. Some municipalities do not submit timely information which results in necessary data adjustments. There is also under-reporting to be considered as well as potential miss-diagnosis given the similarity in clinical symptoms of the viruses (Alvis-Guzmán et al., 2017).

References

Alvis-Guzmán, N., Zakzuk-Sierra, J., Vargas-Moranth, R., Alcocer-Olaciregui, A., Parra-Padilla, D., 2017. Dengue: chikunguña y zika en Colombia 2015–2016. Rev. MVZ Córdoba 22 (Suppl), 5994–6003.

Amin, R., Hendryx, M., Shull, M., Bohnert, A., 2014. A cluster analysis of pediatric cancer incidence rates in Florida: 2000–2010. Stat. Public Policy 1 (1), 69–77.

Bailey, T.C., Gatrell, A.C., 1995. Interactive Spatial Data Analysis, vol. 413 Longman Scientific & Technical, Essex.

Banu, S., Hu, W., Hurst, C., Guo, Y., Islam, M.Z., Tong, S., 2012. Space-time clusters of dengue fever in Bangladesh. Trop. Med. Int. Health 17 (9), 1086–1091.

Banu, S., Hu, W., Guo, Y., Naish, S., Tong, S., 2014. Dynamic spatiotemporal trends of dengue transmission in the Asia-Pacific region, 1955–2004. PLoS One 9 (2), e89440.

Beckham, J.D., Tyler, K.L., 2015. Arbovirus infections. Continuum. (Minneapolis, minn.) 21 (6), 1599 Neuroinfectious Disease.

Benedict, M.Q., Levine, R.S., Hawley, W.A., Lounibos, L.P., 2007. Spread of the tiger: global risk of invasion by the mosquito Aedes albopictus. Vector-Borne Zoonotic Dis. 7 (1), 76–85.

Bhatt, S., et al., 2013. The global distribution and burden of dengue. Nature 496 (7446), 504–507.

Bloch, D., 2016. The Cost and Burden of Chikungunya in the Americas. Public Health Theses. https://elischolar.library.yale.edu/ysphtdl/1022/?utm_source=elischolar.library.yale\.edu%2Fysphtdl%2F1022&utm_medium=PDF&utm_campaign=PDFCoverPages.

Brunsdon, C., Corcoran, J., Higgs, G., 2007. Visualising space and time in crime patterns: a comparison of methods computers. Environ. Urban Syst. 31 (1), 52–75.

Cali, S., 2010. Historia del dengue en Cali. Endemia o una continua epidemia. Secretaria de Salud Publica Municipal de Cali, Cali.

Chachareros, 2015. Cerca de 80000 casos de Chikunguña en Colombia La Cháchara. Colombia.

Charrel, R.N., de Lamballerie, X., Raoult, D., 2007. Chikungunya outbreaks-the globalization of vector borne diseases. N. Engl. J. Med. 356 (8), 769.

Cheng, T., Wicks, T., 2014. Event detection using twitter: a spatio-temporal approach. PLoS One 9 (6), e97807.

Cheng, T., Williams, D., 2012. Space-time analysis of crime patterns in central London. Int. Arch. Photogramm. Remote Sens. Spat. Inf. Sci. 39, 47–52.

Chouin-Carneiro, T., et al., 2016. Differential susceptibilities of aedes aegypti and aedes albopictus from the Americas to Zika virus. PLoS Negl. Trop. Dis. 10 (3), e0004543.

Coleman, M., Coleman, M., Mabuza, A.M., Kok, G., Coetzee, M., Durrheim, D.N., 2009. Using the SaTScan method to detect local malaria clusters for guiding malaria control programmes. Malar. J. 8, 68.

Dejnirattisai, W., et al., 2016. Dengue virus sero-cross-reactivity drives antibody-dependent enhancement of infection with zika virus. Nat. Immunol. 17 (9), 1102–1108.

Delmelle, E., Casas, I., Rojas, J.H., Varela, A., 2013. Spatio-temporal patterns of dengue fever in cali, Colombia. Int. J. Appl. Geospat. Res. (IJAGR) 4 (4), 58–75.

Delmelle, E., Dony, C., Casas, I., Jia, M., Tang, W., 2014. Visualizing the impact of space-time uncertainties on dengue fever patterns. Int. J. Geogr. Inf. Sci. 28 (5), 1107–1127.

Duczmal, L., Assuncao, R., 2004. A simulated annealing strategy for the detection of arbitrarily shaped spatial clusters. Comput. Stat. Data Anal. 45 (2), 269–286.

Durbin, A.P., 2016. Dengue antibody and Zika: friend or foe? Trends Immunol. 37 (10), 635–636.

EPS C, 2015. El incremento del chikunguña es normal. Asi se comparta el virus. Boletin de Prensa COOMEVA EPS. No. 005-2015-1.

Eastin, M.D., Delmelle, E., Casas, I., Wexler, J., Self, C., 2014. Intra-and interseasonal autoregressive prediction of dengue outbreaks using local weather and regional climate for a tropical environment in Colombia. Am. J. Trop. Med. Hyg. 91 (3), 598–610.

Eisen, L., Eisen, R.J., 2011. Using geographic information systems and decision support systems for the prediction, prevention, and control of vector-borne diseases. Annu. Rev. Entomol. 56, 41–61.

Eisen, L., Lozano-Fuentes, S., 2009. Use of mapping and spatial and space-time modeling approaches in operational control of Aedes aegypti and dengue. PLoS Negl. Trop. Dis. 3 (4), e411.

Floore, T.G., 2006. Mosquito larval control practices: past and present. J. Am. Mosq. Control Assoc. 22 (3), 527–533.

Furuya-Kanamori, L., et al., 2016. Co-distribution and co-Infection of chikungunya and dengue viruses. BMC Infect. Dis. 16 (1). http://dx.doi.org/10.1186/s12879-016-1417-2.

Gaudart, J., et al., 2006. Space-time clustering of childhood malaria at the household level: a dynamic cohort in a Mali village. BMC Public Health 6 (1), 286.

Gratz, N.G., 2004. Critical review of the vector status of Aedes albopictus. Med. Vet. Entomol. 18 (3), 215–227.

Greene, S.K., Huang, J., Abrams, A.M., Gilliss, D., Reed, M., Platt, R., et al., 2012.

Gastrointestinal disease outbreak detection using multiple data streams from electronic medical records. Foodborne Pathog. Dis. 9 (5), 431–441.
Hanley, K.A. Han, Weaver, S.C., 2008. Arbovirus Evolution. Origin and Evolution of Viruses. Elsevier, Oxford, pp. 351–392.
Harrington, L.C., Edman, J.D., Scott, T.W., 2001. Why do female Aedes aegypti (Diptera: culicidae) feed preferentially and frequently on human blood? J. Med. Entomol. 38 (3), 411–422.
Hay, S.I., et al., 2013. Global mapping of infectious disease. Philos. Trans. R. Soc. B 368 (1614), 20120250.
Hii, Y.L., Zaki, R.A., Aghamohammadi, N., Rocklöv, J., 2016. Research on climate and dengue in Malaysia: a systematic review. Curr. Environ. Health Rep. 3 (1), 81–90.
Hohl, A., Delmelle, E., Tang, W., Casas, I., 2016. Accelerating the discovery of space-time patterns of infectious diseases using parallel computing. Spat. Spat.-Temp. Epidemiol. 19, 10–20.
INS, 2016a. In: Sivigila, E. (Ed.), Manual del usuario sistema aplicativo SIVIGILA. INS, Colombia. http://www.ins.gov.co/lineas-de-accion/Subdireccion-Vigilancia/sivigila/Documentos SIVIGILA/_ManualSivigila2017.pdf.
INS (Ed.), 2016. Vigilancia Rutinaria por Evento Municipal. INS, Colombia. http://www.ins.gov.co/lineas-de-accion/Subdireccion-Vigilancia/sivigila/Paginas/vigilancia-rutinaria.aspx.
INS, 2017a. Protocolo para la vigilancia en salud pública del dengue. PAHO. http://www.ins.gov.co/lineas-de-accion/Subdireccion-Vigilancia/sivigila/Paginas/vigilancia-rutinaria.aspx.
INS, 2017b. Protocolo de vigilancia en salud pública Chikunguña. INS. http://www.ins.gov.co/lineas-de-accion/Subdireccion-Vigilancia/sivigila/Protocolos SIVIGILA/PRO Chikungunya.pdf.
Jacquez, G.M., Greiling, D.A., Kaufmann, A.M., 2005. Design and implementation of a Space-Time Intelligence System for disease surveillance. J. Geogr. Syst. 7 (1), 7–23.
Jonsson, M.E., Heier, B.T., Norström, M., Hofshagen, M., 2010. Analysis of simultaneous space-time clusters of *Campylobacter* spp. in humans and in broiler flocks using a multiple dataset approach. J. Health Geogr. 9 (1), 48.
Kawiecki, A.B., Christofferson, R.C., 2016. Zika virus–induced antibody response enhances dengue virus serotype 2 replication In vitro. J. Infect. Dis. 214 (9), 1357–1360.
Kitron, U., 1998. Landscape ecology and epidemiology of vector-borne diseases: tools for spatial analysis. J. Med. Entomol. 35 (4), 435–445.
Kitron, U., 2000. Risk maps: transmission and burden of vector-borne diseases. Parasitol. Today 16 (8), 324–325.
Kulldorff, M., Hjalmars, U., 1999. The Knox method and other tests for space-time interaction. Biometrics 55, 544–552.
Kulldorff, M., Heffernan, R., Hartman, J., Assunção, R., Mostashari, F., 2005. A space–-time permutation scan statistic for disease outbreak detection. PLoS Med. 2 (3), e59.
Kulldorff, M., Mostashari, F., Duczmal, L., Katherine Yih, W., Kleinman, K., Platt, R., 2007. Multivariate scan statistics for disease surveillance. Stat. Med. 26 (8), 1824–1833.
Leparc-Goffart, I., Nougairede, A., Cassadou, S., Prat, C., De Lamballerie, X., 2014. Chikungunya in the Americas. Lancet 383 (9916), 514.
Li, Z., et al., 2012. Spatiotemporal analysis of indigenous and imported dengue fever cases in Guangdong province, China. BMC Infect. Dis. 12 (1), 132.
Li, J., et al., 2014. Spatial and temporal emergence pattern of lyme disease in virginia. Trop. Med. Hyg. 91, 1166–1172.
Lian, M., Warner, R.D., Alexander, J.L., Dixon, K.R., 2007. Using geographic information systems and spatial and space-time scan statistics for a population-based risk analysis of the 2002 equine West Nile epidemic in six contiguous regions of Texas. Int. J. Health Geogr. 6 (1), 42.
Liu-Helmersson, J., Stenlund, H., Wilder-Smith, A., Rocklöv, J., 2014. Vectorial capacity of Aedes aegypti: effects of temperature and implications for global dengue epidemic potential. PLoS One 9 (3), e89783.
Métras, R., Porphyre, T., Pfeiffer, D.U., Kemp, A., Thompson, P.N., Collins, L.M., White, R.G., 2012. Exploratory space-time analyses of rift valley fever in South Africa in 2008–2011. PLoS Negl.Trop. Dis. 6 (8), e180.
Mantel, N., 1967. The detection of disease clustering and a generalized regression approach. Cancer Res. 27, 209–220.
Mulatti, P., Mazzucato, M., Montarsi, F., Ciocchetta, S., Capelli, G., Bonfanti, L., Marangon, S., 2015. Retrospective space–time analysis methods to support West Nile virus surveillance activities. Epidemiol. Infect. 143 (1), 202–213.
Naish, S., Hu, W., Mengersen, K., Tong, S., 2011. Spatial and temporal clusters of Barmah Forest virus disease in Queensland, Australia. Trop. Med. Int. Health 16 (7), 884–893.
Nakaya, T., Yano, K., 2010. Visualising crime clusters in a space-time cube: an exploratory data-analysis approach using space-time kernel density estimation and scan statistics. Trans. GIS 14, 223–239.
Noticiascaracol, 2016. Valle aporta el 25% de los casos de dengue en Colombia: Secretaría de Salud. Noticias Caracol. . NoticiasCaracol.com.
Nsoesie, E.O., et al., 2015. Spatial and temporal clustering of chikungunya virus transmission in Dominica. PLoS Negl. Trop. Dis. 9, e0003977.
Ochieng, C., et al., 2013. Mosquito-borne arbovirus surveillance at selected sites in diverse ecological zones of Kenya; 2007–2012. Virol. J. 10 (1), 140.
Ooi, E.E., Goh, K.T., Gubler, D.J., 2006. Dengue prevention and 35 years of vector control in Singapore. Emerg. Infect. Dis. 12 (6), 887.
Paupy, C., et al., 2010. Comparative role of Aedes albopictus and Aedes aegypti in the emergence of Dengue and Chikungunya in central Africa. Vector-Borne Zoonotic Dis. 10 (3), 259–266.
Perez, A., Alkhamis, M., Carlsson, U., Brito, B., Carrasco-Medanic, R., Whedbee, Z., Willeberg, P., 2011. Global animal disease surveillance. Spat. Spatio-Temporal Epidemiol. 2 (3), 135–145.
Peterson, A.T., 2014. Mapping Disease Transmission Risk: Geographic and Ecological Contexts. Johns Hopkins University Press.
Pigott, D.M., et al., 2015. Prioritising infectious disease mapping. PLoS Negl. Trop. Dis. 9 (6), e0003756.
Powell, J.R., Tabachnick, W.J., 2013. History of domestication and spread of Aedes aegypti-a review. Mem. Inst. Oswaldo Cruz 108, 11–17.
Rochlin, I., Ninivaggi, D.V., Hutchinson, M.L., Farajollahi, A., 2013. Climate change and range expansion of the Asian tiger mosquito (Aedes albopictus) in Northeastern USA: implications for public health practitioners. PLoS One 8 (4), e60874.
Rodriguez-Morales, A.J., Villamil-Gómez, W.E., Franco-Paredes, C., 2016. The arboviral burden of disease caused by co-circulation and co-infection of dengue, chikungunya and Zika in the Americas. Travel Med. Infect Dis. 14 (3), 177–179.
Rogerson, P., Yamada, I., 2008. Statistical Detection and Surveillance of Geographic Clusters. CRC Press.
Schmidt, W.P., et al., 2011. Population density, water supply, and the risk of dengue fever in Vietnam: cohort study and spatial analysis. PLoS Med. 8 (8), e1001082.
Shepard, D.S., et al., 2014. Approaches to refining estimates of global burden and economics of dengue. PLoS Negl.Trop. Dis. 8 (11), e3306.
Shepard, D.S., 2010. Cost and burden of dengue and chikungunya from the Americas to asia. Dengue Bull. http://apps.who.int/iris/bitstream/10665/170991/1/db2010v34p1.pdf.
Silva, M.M., et al., 2016. Accuracy of dengue reporting by national surveillance system, Brazil. Emerg. Infect. Dis. 22 (2), 336.
Silverman, B.W., 1986. Density Estimation for Statistics and Data Analysis 26 CRC press.
Tango, T., Takahashi, K., 2005. A flexibly shaped spatial scan statistic for detecting clusters. Int. J. Health Geogr. 4 (1), 11.
Tauil, P.L., 2001. Urbanization and dengue ecology. Cadernos de saúde pública 17, S99–S102.
Theophilides, C.N., Ahearn, S.C., Grady, S., Merlino, M., 2003. Identifying West Nile virus risk areas: the dynamic continuous-area space-time system. Am. J. Epidemiol. 157 (9), 843–854.
Tsetsarkin, K.A., Vanlandingham, D.L., McGee, C.E., Higgs, S., 2007. A single mutation in chikungunya virus affects vector specificity and epidemic potential. PLoS Pathog. 3 (12), e201.
Uittenbogaard, A., Ceccato, V., 2012. Space-time clusters of crime in Stockholm, Sweden. Rev. Eur. Stud. 4 (5), 148.
Ullah, S., Daud, H., Dass, S.C., Khan, H.N., Khalil, A., 2017. Detecting space-time disease clusters with arbitrary shapes and sizes using a co-clustering approach. Geospat. Health 12 (2).
Wang, J., Cao, Z., Zeng, D.D., Wang, Q., Wang, X., Qian (2014), H., 2014. Epidemiological analysis, detection, and comparison of space-time patterns of Beijing hand-foot-mouth disease (2008–2012). PLoS One 9 (3), e92745.
Wang, H., et al., 2016. Global, regional, and national life expectancy, all-cause mortality, and cause-specific mortality for 249 causes of death, 1980–2015: a systematic analysis for the global burden of disease study 2015. Lancet 388 (10053), 1459–1544.
Wilder-Smith, A., Gubler, D.J., Weaver, S.C., Monath, T.P., Heymann, D.L., Scott, T.W., 2017. Epidemic arboviral diseases: priorities for research and public health. Lancet Infect. Dis. 17 (3), e101–e106.
World Health Organization, 2014a. A Global Brief on Vector-Borne Diseases. World Health Organization, pp. 9 WHO/DCO/WHD/2014.1.
World Health Organization, 2014b. “WHO Factsheet Vector-Borne Diseases.” Factsheet Number 387. no. March: 10. http://www.who.int/kobe_centre/mediacentre/vbdfactsheet.pdf.
de Melo, D.P.O., Scherrer, L.R., Eiras, A.E., 2012. Dengue fever occurrence and vector detection by larval survey, ovitrap and MosquiTRAP: a space-time clusters analysis. PLoS One 7 (7), e42125.